Light Mesons and Charm Decays: New Results from E791

Carla Göbel †
Instituto de Física, F. Ing., Univ. República, Montevideo, Uruguay

† on behalf of the E791 Collaboration

Abstract

We will discuss how the decays of charm mesons can be used to study light mesons spectroscopy, by presenting recent results of Dalitz plot analyses using data from Fermilab experiment E791. Emphasis will be on scalar mesons, which are found to have large contribution to the D decays studied. In addition to the usual extraction of decay fractions and relative phases of the intermediate amplitudes, the Dalitz plot technique is used to measure masses and widths of scalar resonances. From the D_s decay, we obtain masses and widths of $f_0(980)$ and $f_0(1370)$. We find evidence for a light and broad scalar resonance, the σ meson, in $D^+ \to \pi^-\pi^+\pi^+$ decay. Preliminary studies also show evidence for a light and broad resonance, the κ meson, in $D^+ \to K^-\pi^+\pi^+$ decay. These results illustrate the potential of charm decays as a laboratory for the study of light mesons.

1 Introduction

The decays of D mesons can be seen as a new environment for the study of light meson physics, due to the high quality of the current samples, the fact that the initial state is always well defined (defined mass, 0^- state), and usually with a small non-resonant contribution. Particularly, these decays can shed light on the scalar mesons, some of them long-standing sources of uncertainty.

Here we present results for the Dalitz plot analyses of the decays $D_s^+ \to \pi^-\pi^+\pi^+$ [1] and $D^+ \to \pi^-\pi^+\pi^+$ [2], and also preliminary results for the decay $D^+ \to K^-\pi^+\pi^+$, using data from the Fermilab E791 experiment[1].

In the $D_s^+ \to \pi^-\pi^+\pi^+$ decay, previous measurements showed the dominance of scalar resonant states[4, 5]. For instance, the decay $f_0(980)\pi^+$ seems to contribute most. Nevertheless, the nature of the $f_0(980)$ is still a puzzle, and in particular its width is poorly measured[6]. From the E791 Dalitz plot analysis

[1] E791 ran in 91-92 with a 500 GeV/c π^- beam. See [3].

of the $D_s^+ \to \pi^-\pi^+\pi^+$ decays, we are able to obtain measurements for the mass and width of this state, as well as for the $f_0(1370)$. For the $D^+ \to \pi^-\pi^+\pi^+$ decay, we are not able to get a good description of the data using the same intermediate states as for $D_s^+ \to \pi^-\pi^+\pi^+$. We find strong evidence for a new light and broad scalar resonance, the $\sigma(500)$, and measure its mass and width. The $D^+ \to \sigma\pi^+$ channel accounts for about half of the total $D^+ \to \pi^-\pi^+\pi^+$ decay rate. Other experiments have presented inconsistent evidence for low-mass $\pi\pi$ resonances in partial wave analyses [7], resulting in ambiguous results for the characteristics of such particles [6, 8].

For the $D^+ \to K^-\pi^+\pi^+$ decay, we present preliminary results from a high statistics sample (almost 23,000 decays). Like previous results for this channel[9, 10] we find that the non-resonant decay is dominant, which is unusual in D decays, but also find important discrepancies between fit model and data. By including a new scalar state, with unconstrained mass and width, we get a much better description of the data. This resonance appears as light and broad according to the fit. Present discussions about the existence of such a state, referred to as the κ in the literature, are very controversial[11].

2 $D^+, D_s^+ \to \pi^-\pi^+\pi^+$ Dalitz plot analyses

In Fig. 1 we show the $\pi^-\pi^+\pi^+$ invariant mass distribution for the sample collected by E791 after reconstruction and selection criteria [1, 2]. Besides combinatorial background, reflections from the decays $D^+ \to K^-\pi^+\pi^+$, $D^+ \to K^-\pi^+$ (plus one extra track) and $D_s^+ \to \eta'\pi^+$, $\eta' \to \rho^0(770)\gamma$ are all taken into account. The hatched regions in Fig. 1 show the samples used for the Dalitz analyses. There are 937 and 1686 candidate events for D_s^+ and D^+ respectively, with a signal to background ratio of about 2:1.

The Dalitz plot corresponding to $D_s^+ \to \pi^-\pi^+\pi^+$ events is shown in Fig. 2(a). The narrow horizontal and vertical bands at $s_{12} \equiv m^2(\pi_1^-\pi_2^+)$ and $s_{13} \equiv m^2(\pi_1^-\pi_3^+)$ just below 1 GeV$^2/c^4$ correspond to the $f_0(980)\pi^+$ state. At the upper edge of the diagonal, there is another concentration of events centered at $s_{12} \simeq s_{13} \simeq$1.8 GeV$^2/c^4$, corresponding to the $f_2(1270)\pi^+$, $f_0(1370)\pi^+$, and $\rho^0(1450)\pi^+$ contributions. From the $D^+ \to \pi^-\pi^+\pi^+$ Dalitz plot (Fig. 2(b)) we see clearly the bands corresponding to the $\rho^0(770)\pi^+$ and $f_0(980)\pi^+$ channels, and an excess of events at low $\pi^-\pi^+$ invariant-mass squared.

To study the resonant structure of these decays, unbinned maximum likelihood fits are applied to the samples. The Dalitz plot distributions are fitted to a sum of signal and background probability distribution functions (PDFs). For each candidate event, the signal PDF is written as the square of the to-

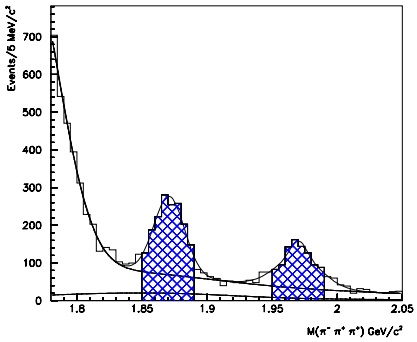

Figure 1: *The $\pi^-\pi^+\pi^+$ invariant mass spectrum. The dotted line represents the $D^0 \to K^-\pi^+$ plus $D_s^+ \to \eta'\pi^+$ reflections and the dashed line is the total background. Events used for the Dalitz analyses are in the hatched areas.*

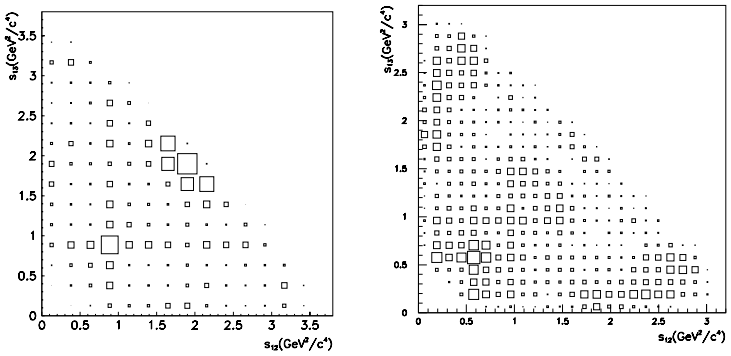

(a) (b)

Figure 2: (a) *The $D_s^+ \to \pi^-\pi^+\pi^+$ Dalitz plot and* (b) *the $D^+ \to \pi^-\pi^+\pi^+$ Dalitz plot. Since there are two identical particles, the plots are symmetrized.*

tal physical amplitude, which is constructed from a coherent sum of Lorentz invariant amplitudes corresponding to the various resonant channels plus the non-resonant decay. The signal PDF is weighted by the acceptance across the Dalitz plot (obtained by Monte Carlo (MC)) and by the level of signal to background for each event, as given by the line shape of Fig. 1.

The resonant channels we include in the fits are $\rho^0(770)\pi^+$, $f_0(980)\pi^+$, $f_2(1270)\pi^+$, $f_0(1370)\pi^+$, and $\rho^0(1450)\pi^+$. We assume the non-resonant amplitude to be uniform across the Dalitz plot. Each resonant amplitude, except that for the $f_0(980)$, is parameterized as a product of form factors, a relativistic Breit-Wigner (B-W) function, and an angular momentum amplitude which

depends on the spin of the resonance,

$$\mathcal{A}_n = \frac{F_D\ F_R\ \mathcal{M}_n^{(J)}}{m_{12}^2 - m_0^2 + im_0\Gamma(m_{12})}\ ,\ \Gamma(m_{12}) = \Gamma_0 \frac{m_0}{m_{12}} \left(\frac{p^*}{p_0^*}\right)^{2J+1} \frac{F_R^2(p^*)}{F_R^2(p_0^*)}\ . \quad (1)$$

Above, m_{12} is the $\pi^+\pi^-$ invariant mass for the candidate resonance. Since there are two like-charge pions, each signal amplitude is Bose-symmetrized, $\mathcal{A}_n = \mathcal{A}_n[(\mathbf{12})\mathbf{3}] + \mathcal{A}_n[(\mathbf{13})\mathbf{2}]$. The quantities F_D and F_R are the Blatt-Weisskopf damping factors [12] respectively for the D and the resonance[2], p^* is the pion momentum in the resonance rest frame at mass m_{12} ($p_0^* = p^*(m_0)$). $\mathcal{M}_n^{(J)}$ describes the angular distribution due to the spin J of the resonance.

For the $f_0(980)\pi^+$ we use a coupled-channel B-W function, following the parameterization of the WA76 Collaboration[13],

$$BW_{f_0(980)} = \frac{1}{m_{\pi\pi}^2 - m_0^2 + im_0(\Gamma_\pi + \Gamma_K)}\ , \quad (2)$$

$$\Gamma_\pi = g_\pi \sqrt{m_{\pi\pi}^2/4 - m_\pi^2},\ \Gamma_K = \frac{g_K}{2}\left(\sqrt{m_{\pi\pi}^2/4 - m_{K^+}^2} + \sqrt{m_{\pi\pi}^2/4 - m_{K^0}^2}\right). \quad (3)$$

We multiply each amplitude by a complex coefficient, $c_n = a_n e^{\delta_n}$. The fit parameters are the magnitudes, a_n, and the phases, δ_n, which accommodate the final state interactions.

2.1 Results for $D_s^+ \to \pi^-\pi^+\pi^+$

The $D_s^+ \to \pi^-\pi^+\pi^+$ Dalitz plot (Fig. 2(a)) is fitted to obtain not only the relative contributions (and phases) of the possible sub-channels, but also the parameters of the $f_0(980)$ state, g_π, g_K, and m_0, as well as the mass and width of the $f_0(1370)$. That is, they are determined directly from the data, as free parameters in the fit. The other resonance masses and widths are taken from the PDG[6]. The resulting fractions and phases are shown in Table 1.

The measured $f_0(980)$ parameters are $m_0 = 977 \pm 3 \pm 2$ MeV/c^2, $g_\pi = 0.09 \pm 0.01 \pm 0.01$ and $g_K = 0.02 \pm 0.04 \pm 0.03$. Our value for g_π is in very good agreement with OPAL and MARKII results [14], but WA76 [13] found a much larger value, $g_\pi = 0.28 \pm 0.04$. Our value of g_K indicates a small coupling of $f_0(980)$ to $K\bar{K}$. The values of the $f_0(980)$ mass and of g_π, as well as the magnitudes and phases of the resonant amplitudes, are relatively insensitive to the value of g_K. Both OPAL and MARKII results are also insensitive to the value of g_K. WA76, on the contrary, measured $g_K = 0.56 \pm 0.18$.

[2]For three pions analyses, the effective radii for F_D and F_R are set to 3.0GeV^{-1}; for the $D^+ \to K^-\pi^+\pi^+$ analysis of section 3, the radii taken for F_D and F_R are respectively 3.0GeV^{-1} and 1.5GeV^{-1}.

Table 1: *Dalitz fit results for* $D_s^+ \to \pi^-\pi^+\pi^+$.

Decay Mode	Phase(°)	Fraction(%)
$f_0(980)\pi^+$	0 (fixed)	$56.5 \pm 4.3 \pm 4.7$
non-reson.	$181 \pm 94 \pm 51$	$0.5 \pm 1.4 \pm 1.7$
$\rho^0(770)\pi^+$	$109 \pm 24 \pm 5$	$5.8 \pm 2.3 \pm 3.7$
$f_2(1270)\pi^+$	$133 \pm 13 \pm 28$	$19.7 \pm 3.3 \pm 0.6$
$f_0(1370)\pi^+$	$198 \pm 19 \pm 27$	$32.4 \pm 7.7 \pm 1.9$
$\rho^0(1450)\pi^+$	$162 \pm 26 \pm 17$	$4.4 \pm 2.1 \pm 0.2$

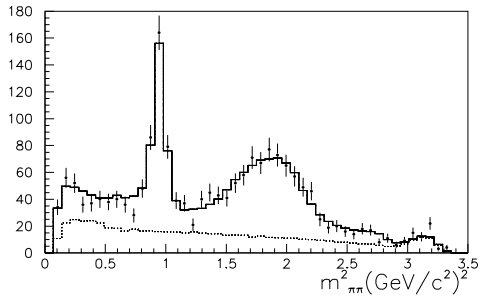

Figure 3: *s_{12} and s_{13} ($m^2_{\pi\pi}$) projections for $D_s^+ \to \pi^-\pi^+\pi^+$ data (dots) and our best fit (solid). The hashed area corresponds to background.*

We have also fit the Dalitz plot using for the $f_0(980)$ the same B-W function as for the other resonances. We find $m_0 = 975 \pm 3$ MeV/c^2 and $\Gamma_0 = 44 \pm 2 \pm 2$ MeV/c^2, and the results for fractions and phases are indistinguishable.

A χ^2 distribution is produced from the difference in densities for model (from a fast-MC algorithm) and data. From the χ^2 and the number of degrees of freedom (ν), the confidence level of the model is 35% [1]. A visual comparison between the fit model and the data can be seen in Fig. 3 where we show the sum of the s_{12} and s_{13} projections for data (points) and model (solid lines, from fast-MC).

If the $D_s^+ \to \pi^-\pi^+\pi^+$ decay is dominated by the Cabibbo-favored spectator mechanism, we would expect final states with a large $s\bar{s}$ content. As we can see by the results of Table 1, approximately half of the $D_s^+ \to \pi^-\pi^+\pi^+$ rate is produced via $f_0(980)\pi^+$. If the spectator amplitude is dominant in this decay, this would support the interpretation of the $f_0(980)$ as an $s\bar{s}$ state. On the other hand, the large contribution from the intermediate state $f_0(1370)\pi^+$ indicates the presence of either W-annihilation amplitudes or strong rescattering in the final state. In fact, the $f_0(1370)\pi^+$ is not observed in the $D_s^+ \to K^+K^-\pi^+$

final state[15], pointing to the $f_0(1370)$ being a non-$s\bar{s}$ particle, as suggested by the naive quark model[6]. There is no evidence in the D_s^+ decay for a low-mass broad scalar particle as seen in the D^+ decay, discussed below.

2.2 Results for $D^+ \to \pi^-\pi^+\pi^+$

In a first approach, we try to fit the $D^+ \to \pi^-\pi^+\pi^+$ Dalitz plot (Fig. 2(b)) using the same amplitudes used for the $D_s^+ \to \pi^-\pi^+\pi^+$ analysis. We find that, with this model, the non-resonant, the $\rho^0(1450)\pi^+$, and the $\rho^0(770)\pi^+$ amplitudes dominate (results shown on the first column of Table 2), reproducing the same qualitative features from those reported previously [4, 5]. However, this model does not describe the data satisfactorily, especially at low $\pi^-\pi^+$ mass squared, as can be seen from Fig. 4(a). The χ^2/ν obtained from the binned Dalitz plot for this model is 1.6, with a confidence level less than 10^{-5}.

To investigate the possibility that another $\pi^-\pi^+$ resonance contributes to the $D^+ \to \pi^-\pi^+\pi^+$ decay, we add an extra scalar resonance amplitude to the signal PDF. We allow its mass and width to float as free fit parameters.

We find that this model improves our fit substantially, converging to values of mass and width of this scalar resonance, called $\sigma(500)$, of $478^{+24}_{-23}\pm17$ MeV/c^2 and $324^{+42}_{-40}\pm21$ MeV/c^2, respectively. According to this model, this amplitude produces the largest decay fraction, as shown in the second column of Table 2; the non-resonant amplitude, which is dominant in the model without $\sigma\pi^+$, drops substantially. This model describes the data much better, as can be seen by the $\pi\pi$ mass squared projection in Fig. 4(b). The χ^2/ν is now 0.9, with a corresponding confidence level of 91%.

To better understand our data, we also fit it with vector, tensor, and toy models for this extra amplitude, allowing the masses, widths, and relative amplitudes to float freely. The vector and tensor models test the angular distribution of the signal. The toy model tests the phase variation expected from a B-W amplitude by forcing this amplitude to have a constant relative phase but still a B-W shape vs. mass. All these alternative models fail to describe the data as well as the scalar (regular) B-W amplitude (see [2]).

3 Preliminary results for $D^+ \to K^-\pi^+\pi^+$ Dalitz analysis

Previous analyses of the Dalitz plot of the decay $D^+ \to K^-\pi^+\pi^+$ [9, 10] showed the unusual dominance of the non-resonant decay. The most recent result comes from E687 [10] with a sample of about 8000 events, where besides the non-

Table 2: *Dalitz fit results for* $D^+ \to \pi^-\pi^+\pi^+$ *. First errors are statistical, second systematics (only for fit with* $\sigma\pi^+$ *mode).*

Decay Mode	Fit without $\sigma\pi^+$		Fit with $\sigma\pi^+$	
	Phase(°)	Fraction(%)	Phase(°)	Fraction(%)
$\sigma\pi^+$	–	–	$206 \pm 8 \pm 5$	$46.3 \pm 9.0 \pm 2.1$
$\rho^0(770)\pi^+$	0 (fixed)	20.8 ± 2.4	0 (fixed)	$33.6 \pm 3.2 \pm 2.2$
non-reson.	150 ± 12	38.6 ± 9.7	$57 \pm 20 \pm 6$	$7.8 \pm 6.0 \pm 2.7$
$f_0(980)\pi^+$	152 ± 16	7.4 ± 1.4	$165 \pm 11 \pm 3$	$6.2 \pm 1.3 \pm 0.4$
$f_2(1270)\pi^+$	103 ± 16	6.3 ± 1.9	$57 \pm 8 \pm 3$	$19.4 \pm 2.5 \pm 0.4$
$f_0(1370)\pi^+$	143 ± 10	10.7 ± 3.1	$105 \pm 18 \pm 1$	$2.3 \pm 1.5 \pm 0.8$
$\rho^0(1450)\pi^+$	46 ± 15	22.6 ± 3.7	$319 \pm 39 \pm 11$	$0.7 \pm 0.7 \pm 0.3$

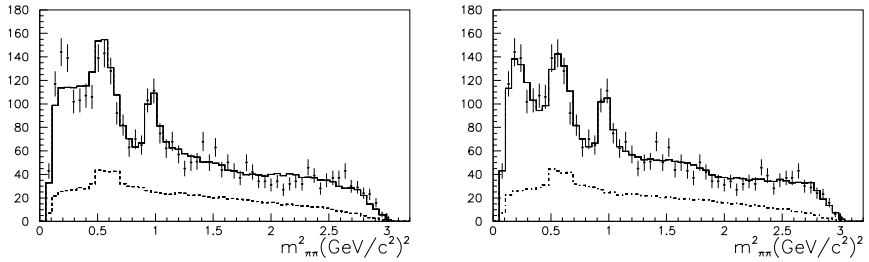

(a) (b)

Figure 4: s_{12} *and* s_{13} *(*$m^2_{\pi\pi}$*) projections for* $D^+ \to \pi^-\pi^+\pi^+$ *data (dots) and our best fit (solid) for models* (a) *without and* (b) *with* $\sigma\pi^+$ *amplitude. The dashed distribution corresponds to the expected background level.*

resonant (about 95% of the decay rate) they find contributions from the channels $\bar{K}^*_0(1430)\pi^+$, $\bar{K}^*(890)\pi^+$, and $\bar{K}^*(1680)\pi^+$. However, they don't obtain a good description of the data, arriving to a χ^2/ν of 3.

In Fig. 5(a) we show the $K^-\pi^+\pi^+$ invariant mass distribution for the sample collected by E791 after reconstruction and selection criteria. Besides combinatorial background, the other main source of background comes from the reflection of the decay $D_s^+ \to K^-K^+\pi^+$ (through $\bar{K}^*K^+$ and $\phi\pi^+$). The total level of background is shown by the filled area in Fig. 5(a). The hashed area corresponds to the sample used for the Dalitz analysis. There are 22890 events in this sample, where about 6% correspond to background.

The Dalitz plot of the signal-region events is shown in Fig. 5(b). The plot presents a rich structure, where we can observe the clear bands from $\bar{K}^*(890)\pi^+$, and an accumulation of events at the upper edge of the diagonal, due to the heavier resonances.

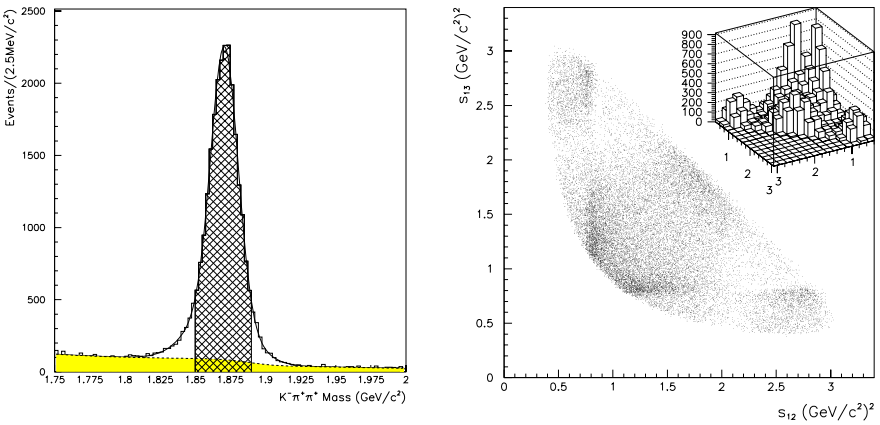

(a) (b)

Figure 5: *(a) The $K\pi\pi$ invariant mass spectrum. The shaded area is background; (b) Dalitz plot corresponding to the events in the dashed area of (a).*

The formalism used for the $D^+ \to K^-\pi^+\pi^+$ Dalitz plot fit is essentially the same as for the D^+, D_s^+ three pions decays[3]. The results presented here are all preliminary, in particular no studies of systematic effects are addressed.

All possible known $K\pi$ resonances [6] are included in the model in a first step. We find significant contributions from the same channels observed previously[9, 10], but with our higher statistics sample we also measure a small but significant contribution from $\bar{K}_2^*(1430)\pi^+$. The decay fractions and phases for this model are shown in Table 3, first column. We confirm the high non-resonant rate (over 100%); there is an impressive interference pattern according to this model, reflected by the sum of the fractions being around 150%.

However, this model does not provide a good description of the data. The calculated χ^2/ν from the binned Dalitz plot distribution is 2.7. By observing the $m^2(K\pi_{low})$ and $m^2(K\pi_{high})$ projections for data (points) and model (solid) in Fig. 6(a), we see discrepancies at low $K\pi$ mass squared (below 0.6 GeV^2/c^4, where data has very small error bars) and also near 2.5 GeV^2/c^4.

The strong evidence for the $\sigma(500)$ from the $D^+ \to \pi^-\pi^+\pi^+$ decay leads us to question whether a new resonance state could be responsible for the difficulty in modeling the $D^+ \to K^-\pi^+\pi^+$ data. The light and broad scalar $K\pi$ resonance, the κ (a σ-meson nonet member), is presently the subject of many discussions, with controversial results from $K\pi$ scattering analyses[16, 11].

[3]Besides the differences in the factor F_R addressed before, here we define the relativistic Breit-Wigner with a factor of (-1) with respect to equation 1, for easier comparison to previous analysis [10].

Table 3: *Dalitz fit results for* $D^+ \to K^-\pi^+\pi^+$. **PRELIMINARY***; statistical errors only.*

Decay Mode	Fit without $\kappa\pi^+$		Fit with $\kappa\pi^+$	
	Phase(°)	Fraction(%)	Phase(°)	Fraction(%)
non-reson.	0 (fixed)	103.9 ± 2.3	0 (fixed)	52.4 ± 8.5
$\kappa\pi^+$	–	–	187 ± 11	20.7 ± 5.4
$\bar{K}^*(890)\pi^+$	51 ± 1	12.7 ± 0.4	15 ± 6	11.3 ± 0.4
$\bar{K}_0^*(1430)\pi^+$	63 ± 1	33.6 ± 1.4	63 ± 5	17.6 ± 1.7
$\bar{K}_2^*(1430)\pi^+$	51 ± 6	0.5 ± 0.1	348 ± 10	0.3 ± 0.1
$\bar{K}^*(1680)\pi^+$	70 ± 3	3.8 ± 0.3	53 ± 6	3.3 ± 0.7

We introduce in our model an extra spin-0 resonant amplitude. Both mass and width of this hypothetical κ state are allowed to float in the fitting procedure. Moreover, since the mass and width of the other scalar resonance, $K_0^*(1430)$, were obtained from the LASS experiment in the absence of this extra amplitude[16], we also allow these parameters to float. The fit converges to values of the κ mass and width of 815 ± 30 MeV/c^2 and 560 ± 116 MeV/c^2 respectively, and to values for the $K_0^*(1430)$ mass and width of 1465 ± 6 MeV/c^2 and 182 ± 10 MeV/c^2 respectively. The results for κ are consistent to this state being a light and broad resonance [11]. The results for the $K_0^*(1430)$ show this state being narrower and heavier than obtained by LASS [6, 16]. The decay fractions and phases from this model are shown in Table 3, second column. The non-resonant fraction drops to about 50% and the $\kappa\pi^+$ accounts for about 20% of the decay, representing the second main contribution, followed by the other scalar state, $\bar{K}_0^*(1430)\pi^+$. The fit quality of this model is considerably superior to the model without the $\kappa\pi^+$ state: the χ^2/ν is now 0.9, the confidence level of the fit is 79%. As can be seen by the projections in Fig. 6(b), there is very good agreement between model and data.

As was done for testing the σ state, we test a variety of other models to check their ability to explain the data. We represent the extra amplitude by vector, tensor and toy (B-W with no phase variation) models, allowing mass and width to float. None of these models reproduced the data as well as the scalar resonance hypothesis.

4 Conclusions

Dalitz plot analyses presented here from E791 data point to the importance of the scalar resonant states in the 3π and $K\pi\pi$ final states of D mesons. From the $D_s^+ \to \pi^-\pi^+\pi^+$ analysis, we find that about 90% of the decay rate is

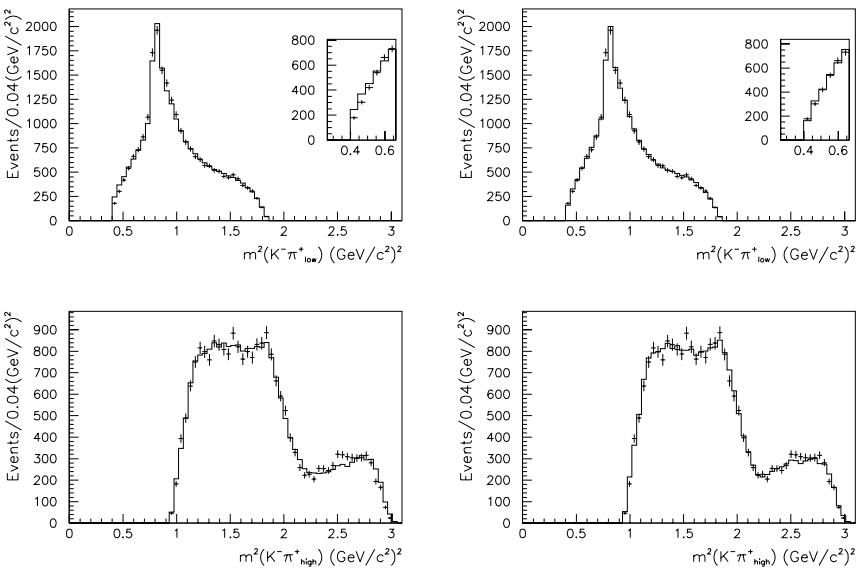

(a) (b)

Figure 6: $m^2(K\pi_{low})$ *and* $m^2(K\pi_{high})$ *projections for* $D^+ \to K^-\pi^+\pi^+$ *data (points) and our best fit (solid) for models* (a) *without and* (b) *with* $\kappa\pi^+$ *state.*

due to $f_0\pi^+$ intermediate states. Almost half of the $D^+ \to \pi^-\pi^+\pi^+$ decay rate proceeds through a new scalar state $\sigma(500)\pi^+$. From $D^+ \to K^-\pi^+\pi^+$ decay, we present evidence for a new scalar state $\kappa\pi^+$ and, although about 50% of the decay rate corresponds to the non-resonant channel, 40% comes from the scalar states. We are able to measure the masses and widths of these scalar resonances. These results illustrate the potential of many-body D meson decays for the study of light-meson spectroscopy.

References

[1] E.M. Aitala *et al.* (E791 Coll.), hep-ex/0007027, accepted by PRL.

[2] E.M. Aitala *et al.* (E791 Coll.), hep-ex/0007028, accepted by PRL.

[3] J. Appel, Ann. Rev. Nucl. Part. Sci. **42**, 367 (1992); D. Summers *et al.*, hep-ex/0009015; S. Amato *et al.*, Nucl. Instr. Meth. A **324**, 535 (1993); E.M. Aitala *et al.* (E791 Coll.), Eur. Phys. J. direct C **4**, 1 (1999).

[4] J.C. Anjos *et al.* (E691 Coll.), Phys. Rev. Lett. **62**, 125 (1989).

[5] P.L. Frabetti *et al.* (E687 Coll.), Phys. Lett. B **407**, 79 (1997).

[6] C. Caso *et al.* (Particle Data Group), Eur. Phys. J. C **15**, 1 (2000).

[7] D. Barberis *et al.* (WA102 Coll.), Phys. Lett. B **453**, 316 (1999); D.M. Asner *et al.* (CLEO Coll.), Phys. Rev. D **61**, 012002 (2000); D. Alde, *et al.* (GAMS Coll.), Phys. Lett. B **397** , 350 (1997).

[8] N. Tornqvist, hep-ph/9904346.

[9] J.C. Anjos *et al.* (E691 Coll.), Phys. Rev. D **48**, 56 (1993).

[10] P.L. Frabetti *et al.* (E687 Coll.), Phys. Lett. B **331**, 217 (1994).

[11] D. Black *et al.*, Phys. Rev. D **58**, 054012 (1998); S. Ishida *et al.*, Prog. Theor. Phys. **98**, 621 (1997); S.N. Cherry and M.R. Pennington, hep-ph/0005208; and references therein.

[12] J. Blatt and V. Weisskopf, Theoretical Nuclear Physics (Wiley, 1962).

[13] T.A. Armstrong *et al.* (WA76 Coll.), Z. Phys. C **51**, 351 (1991).

[14] K. Ackerstaff *et al.* (OPAL Coll.), Eur. Phys. J. C **4**, 19 (1998); G. Gidal *et al.* (MARKII Coll.), Phys. Lett. B **107**, 153 (1981).

[15] P.L. Frabetti *et al.* (E687 Coll.), Phys. Lett. B **351**, 591 (1995).

[16] D. Aston *et al.* (LASS Coll.), Nucl. Phys. B **296**, 493 (1988).